Cell Reports, Volume *22*

Supplemental Information

β-aminoisobutyric Acid, L-BAIBA, Is a Muscle-Derived Osteocyte Survival Factor

Yukiko Kitase, Julian A. Vallejo, William Gutheil, Harika Vemula, Katharina Jähn, Jianxun Yi, Jingsong Zhou, Marco Brotto, and Lynda F. Bonewald

Supplemental Experimental Procedures

C2C12 Cells

C2C12 murine multipotent cells were cultured as previously described (Cai et al., 2009; Shen et al., 1997; Zhao et al., 2008) in DMEM/high glucose +10 % FBS (100 U/mL P/S) and were maintained at 40–70 % cell density in a 5% CO_2 incubator at 37°C.

Testing and characterization of C2C12 myotube conditioned media (MT-CM)

Preparation of MT-CM: C2C12 cells were plated at 6,500 cells/cm^2 in T75 flasks supplemented with 12 mL culture media/ flask. Cells were induced to form MTs by switching culture medium to DMEM + 2.5 % horse serum (100 U/mL P/S) at a cell density of 80–90 % (2-3 day post-seeding). Cells were then cultured for 5–6 day until multinucleated, spontaneously contracting MTs were formed. The CM was generated during a 24 h culture period by changing the culture medium to phenol red-free DMEM/high glucose + 0.1 % BSA (100 U/mL P/S). Prior to use, the produced CM was centrifuged at 500 g for 5 min at 4 °C to remove cells and cellular debris. A similar DNA to culture media volume ratio was achieved using the described methods to generate MT-CM.

Quantification of cell viability: The percentage of cell death was quantified using the trypan blue exclusion method following previously published procedures (Ahuja et al., 2003; Kitase et al., 2010). Briefly, cells were cultured overnight, washed with phosphate-buffered saline (PBS) and treated with or without MT-CM for 1 h at various concentrations using phenol red-free αMEM + 2.5 % FBS + 2.5 % CS (100 U/ mL P/S) as culture medium. After pre-treatment, cells were exposed to phenol red-free culture media with or without 1 μM dexamethasone (Sigma-Aldrich, D4902) for 6 h. Adherent cells were trypsinized and combined with non-adherent cells. Cells were incubated for 10 min with 0.1 % trypan blue (Sigma-Aldrich, T8154). A Neubauer hemocytometer was used to count viable, non-stained cells and dead or dying cells that demonstrate blue staining throughout the whole cell body. Experiments contained 4–6 biological replicates and on average 100 cells per replicate were counted. Also, cellular apoptosis via nuclear fragmentation was performed. Cells were fixed for 10 min at 4 °C in 2 % neutrally buffered paraformaldehyde and after treatment nuclei were stained with 0.25 mg/mL DAPI (Sigma-Aldrich, D9542) for 5 min. The percentage of apoptotic cells was determined counting cells with an impaired nuclear membrane that demonstrate nuclear blebbing *versus* non-impaired cells. Experiments contained 4–6 biological replicates and an average 100 cells per replicate were counted.

Size cutoff: Amicon® Ultra-4 Centrifugal Filter Units for i) 10kD (Merck, UFC801008) and ii) 3kD (Merck, UFC800308) were used according to manufacturer's instructions. MT-CM was separated at 2750 g, 4° C for 45 min -2h in a swing rotor centrifuge until $\geq$ 85% of the volume was filtrated. 10% of the filtrate and retentate were used for experiments (see above).

Trypsin digest: Trypsin digest was performed overnight at 37°C with 0.05% Trypsin (Sigma-Aldrich, T4799) added. The successful digest was verified by SDS-PAGE and digested MT-CM was used at 10% for viability experiments (see above).

UV: UV light exposure was done using the cell culture hood UV light. MT-CM was placed into a tissue culture plastic dish and exposed to UV light for 24 h at RT. Exposure to RT for 24 h without UV light does not affect the stability of MT factor (data not shown). UV-exposed MT-CM was used at 1% for viability experiments (see above).

Heat/Boiling: Exposure to heat was done in a water bath set to 100°C. MT-CM in a sealed container was brought to a boiling state for 15 min, cooled down to RT and used at 1% for viability experiments (see above).

Quantification of reactive oxygen species (ROS)

MLO-Y4 cells were plated at 1×10^4/cm^2 on a collagen-coated 96-well plate with 8 wells for each experimental condition. Representative examples of three independent experiments are shown. Cells were pretreated with varying concentrations of L-BAIBA in 0.5% FBS/ 0.5% CS/α-MEM for 1 h, followed by treatment with 0.3 mM hydrogen peroxide for 1 h in 0.5% FBS/ 0.5% CS/α-MEM to induce cell death. Cells were stained with 5 μM CellROX orange reagent (Molecular probe, C10443) for 30 min to detect cellular oxidative stress. CellROX orange fluorescence dye is non-fluorescent while in a reduced state but starts to exhibit bright orange fluorescence upon oxidation by ROS. Images were obtained using the Nikon fluorescence microscope and quantified signal intensity using ImageJ. Integrated Density obtained from thresholded images was normalized by cell number. The signal intensity was presented as fold change based on the value in control sample.

Micro-computed tomography

In vivo μCT images were taken to assess the changes of bone structure at two-time points, 2 days before hindlimb unloading as a baseline and 2 days before sacrifice as the endpoint. Mice were anesthetized with 75mg/kg ketamine/0.5mg/kg Dex-Dormitor and right tibia was scanned by X-ray μCT (vivaCT40; Scanco Medical AG) at 55 kV, 145 μA, high resolution, 19 mm voxel, 200 ms integration time. To confirm the results of *in vivo* μCT, *ex vivo* μCT was also conducted using the same right tibiae. The tibiae were dissected and fixed for 1 day in 4% paraformaldehyde, and then kept in 70% ethanol at 4C until use. Specimens were scanned at 55 kV, 145 μA, high resolution, 10.5 mm voxel, 200 ms integration time. Three-dimensional images reconstructed within the range of 1 mm from the most proximal metaphysis of tibiae were analyzed. Trabecular morphometry was studied by excluding the cortical bone from the endocortical borders using hand-drawn contours followed by thresholding (sigma=0.8, support=1, lower/upper threshold=245/1000=332 mg HA/cm^3, peel iteration=0), and was characterized by bone volume fraction (BV/TV), trabecular number (Tb.N), trabecular thickness (Tb.Th), trabecular spacing (Tb.Sp), and connectivity density (Conn.D). Changes in the trabecular parameters in *in vivo* μCT images were expressed as a percentage of the baseline.

Structure model index (SMI) has been frequently used as a method to determine the rod-or plate-like geometry of trabecular structures (Hildebrand and Ruegsegger, 1997) but Ellipsoid factor (EF) classification was introduced recently to replace the SMI (Salmon et al., 2015). EF classification was performed using *ex vivo* μCT binary images with the range of 0.1-0.6 mm from the most proximal metaphysis of tibiae and analyzed with ImageJ plugins, BoneJ (Doube et al., 2010) and 3D viewer (Schmid et al., 2010) to visualize three-dimensionally. EF images and histograms were obtained using the following sampling options. Sampling increment: 0.001mm, Vectors: 20, Skeleton points per ellipsoid: 1, Contact sensitivity: 10, Maximum interactions: 20 and Maximum drift: 0.02 that allows 90% of pixels classified by at least one ellipsoid. EF images contain EF values ranging from -1 (most oblate, black color) to +1 (most prolate, white color).

Bone Histomorphometry

Left tibiae were fixed with 4% paraformaldehyde at 4°C for 1 day and then demineralized in 10% EDTA/PBS pH7.4. The bones were subsequently washed with PBS and dehydrated in different ethanol baths for 4hr each. Bones were then paraffin embedded and paraffin sections (5 μm) were cut, dewaxed, rehydrated. To visualize osteoclasts sections were stained for TRAP using a modification of Erlebacher and Derynck (Erlebacher and Derynck, 1996). The modifications consisted of (1) substituting Fast Red TR 1,5-napthalenedisulfonate salt for the chromophore and (2) increasing the incubation period. The TRAP reaction was counterstained with toluidine blue in Sorenson's buffer (Stevens and Farncis, 1996) to reveal osteoid and osteoblasts. Bone histomorphometric parameters were evaluated using Osteomeasure software (OsteoMetrics, Inc.). The region of interest analyzed was 1 mm in length, 200μm below the growth plate, corresponding to the area analyzed by μCT on the contralateral tibia. Osteocyte apoptosis was detected by TdT-mediated dUTP nick-end labeling (TUNEL) using a modified version of a commercial kit (GeneCopoeia). The modifications comprised (1) exposing the sections after de-parafinization and rehydration to 10 mM citrate buffer (pH 6.0) for 5 minutes at 48° C and (2) permeabilization using 0.05% pepsin in 0.1N HCL for 4 minutes at 37°C. The TUNEL reaction was counterstained using 0.2% methyl green. TUNEL negative osteocytes were quantified to examine the osteocyte viability *in vivo.*

Ex vivo muscle contractility analysis

Mice were sacrificed by cervical dislocation after collecting blood samples and the EDL and soleus muscles were removed for contractility analysis as previously described (Thornton et al., 2011). Muscles were immediately placed into a dish containing a physiological buffer solution (144 mM NaCl; 5 mM KCl; 1 mM $MgCl_2$; 25 mM $NaHCO_3$; 2.5 mM $CaCl_2$; pH 7.40) with 10 mM glucose. This solution was continuously aerated with a 95/5% O_2/CO_2 mixture. EDL and soleus muscles were mounted vertically between two stimulating platinum electrodes and proximal and distal tendons were secured to adjustable isometric force transducers and to a fixed support, respectively. The muscles were immersed into 20 mL bathing chambers containing an oxygenated physiological buffer. PowerLab® Software (ADInstruments Inc.) was used to store and analyze force data. Stimulatory voltage was provided by an S88X dual pulse digital stimulator (Grass Products) (100 V, pulse duration, 1 ms; train duration, 500 ms). Muscles were lengthened until a single tetanus stimulation produced maximal force and remained at this optimal muscle length (L_0) for the duration of the experiment. The bathing solution was then increased to 37°C and maintained at this temperature by a heated water circulating pump. All data are presented as mean ± SD.

Equilibration: EDL and soleus muscles were next allowed a 30 min equilibration period during which time they were stimulated with intercalating high and low-frequency pulse trains spaced every 3 min which corresponded to maximal (T_{max}) and half maximal (½ T_{max}) isometric force, respectively (200/100Hz for EDL; 160/40Hz for soleus). The proposed stimulation protocol

aids with the study of the relative contributions of the contractile machinery (T_{max}) and the EC-coupling (½ T_{max}) to contractile function (Brotto et al., 2002; Thornton et al., 2011).

Force-Frequency Relationship: Following equilibration, the EDL and soleus muscles were stimulated to contract with frequencies ranging from 1-200 Hz with a periodicity of 3 min to generate the force vs. frequency (FF) relationship.

Force data: Muscle force is reported as absolute force (mN) and force normalized to the following muscle physiological cross-sectional area (PCSA, N/cm^2) equation as previously reported (de Paula Brotto et al., 2001; Park et al., 2012), with a small modification, in that, in our final length calculation we considered the length to ratio of muscle fibers for stretched muscles (tendon-to-tendon) of ex vivo muscles in contractility chambers. We used the previous factors reported for EDL (0.75) and SOL (0.85) by James et al (1995), which has also been consistently used by Talis and colleagues (Tallis et al., 2014; Tallis et al., 2017) . It essentially means that the actual muscle fiber size is smaller than the length of the measured stretched muscle. Since the PCSA is very sensitive to length, by adjusting to the length of the muscle fiber, force estimation is more precise. Thus, our final formula was:

Muscle force (N/cm^2) = (force (g) x (muscle length (cm) x 0.75 (EDL) or 0.85 (SOL) x 1.06 (muscle density))/ (muscle weight (g) x 0.00981).

Importantly, our normalized forces are well within the upper levels of forces reported by other groups when experiments are performed at 37ºC (Bonetto et al., 2015; James et al., 2013; Tallis et al., 2017; Wright et al., 2017).

Slope data: The slope of the rising edge of muscle contractions was measured 0-31 ms after the start of the peak.

Measurement of BAIBA in muscle conditioned media (CM)

Preparation of muscle CM: Muscle CM were prepared from intact EDL and soleus muscles dissected from 5- or 22-month-old C57BL/6 male (n=5 for each age group) and female (n=6 and 4 for each age group respectively) mice. Muscles were placed inside Radnotti Chambers containing 20 mL of Ringer's solution using a four-chamber system driven by an ADI-PowerLab Software. The experimental condition previously defined (Jahn et al., 2012) was used in this study with some modifications. Briefly, static CM was obtained by placing muscles in the chamber without stimulation for 30min. Next, the optimal length of muscle allowing it to achieve maximal force was determined by the length-force relationship followed by 30 min equilibration. The force *versus* frequency relationship was conducted by stimulating with frequencies ranging from 1–130 Hz. Muscles were then equilibrated with stimulatory trains of 500 ms, 90 Hz, repeated at every minute for 30 min to collect muscle CM 90 Hz.

Quantification of BAIBA in muscle CM: D- and L-BAIBA levels in muscle CM were quantified using our previously described multichannel LC-MS/MS approach (Vemula et al., 2017). Briefly, to 1 mL of muscle CM was added 3 µL of 10 µM D-alanine (Sigma-Aldrich, A7377) as an internal standard, and protein precipitated with 2 volumes of ice-cold acetone (Fisher Scientific). After 10 min on ice, the sample was centrifuged at 3000 g, and the supernatant was collected, freeze-dried, and redissolved in 50 µL of HPLC water (Alfa Aesar)/0.1% formic acid (Fisher Scientific). A 20 µL aliquot of this reconstituted sample was derivatized with 20 µL of 40 mM Marfey's reagent (Novabiochem) in acetone plus 5 µL of 1 M triethylamine (Fisher Scientific) in water. This Marfey's derivatization reaction was incubated at 37 ºC for 2.5 h, and the reaction quenched by adding 5 µL of 1 M HCl and 150 µL of HPLC water/25% acetonitrile (Alfa Aesar) /0.1% formic acid. Derivatized samples were then analyzed for D- and L-BAIBA levels by liquid chromatography-mass spectrometry (LC/MS) as described in detail previously (Vemula et al, 2017). In comparison with other isobaric (same mass) aminobutyric acid isomers which all have a parent ion (Q1) at 356.2 m/z in positive mode, Marfey's-BAIBA derivatives provide a characteristic fragment (Q3) at 192.2 m/z, which is unique to D- and L-BAIBA isomers.

Quantification of amino acids in muscle CM: Amino acid levels in EDL and SOL male muscle CM were determined using Marfey's derivatized samples by LC-MS/MS quantification as described previously (Bobba et al., 2012; Jamindar and Gutheil, 2010; Putty et al., 2011; Putty et al., 2013). The amino acid concentration was obtained by subtracting the values in Ringer buffer.

Real-time quantitative PCR (RT-qPCR)

Preparation of mouse long bones: Long bones were dissected from 2.5-, 5- and 22-month-old male (n=3, 5 and 3 for each age group respectively) and female (n=4, 5 and 5 for each age group respectively) mice. Osteocyte-enriched long bones and osteoblast fractions were obtained as described in the above. Femurs obtained from hindlimb-unloaded male mice were flushed

to remove bone marrow but not digested with a series of collagenase/EDTA to examine differential gene expressions as a whole bone. Bones were pulverized using Bessman Tissue Pulverizer chilled with liquid nitrogen.

Preparation of MLO-Y4 cells: MLO-Y4 cells were plated at $1\times10^4/cm^2$ on a collagen-coated 6-well plate (3-4 replicates per treatment). For examining receptor expression levels, the cells were harvested next day. For examining mitochondrial gene expression levels, the cells were pretreated with L-BAIBA in 0.5% FBS/ 0.5% CS/α-MEM for 1 h, followed by treatment with 0.3 mM hydrogen peroxide for 1 h in 0.5% FBS/ 0.5% CS/α-MEM to induce cell death.

Total RNA extractions were carried out using TRIzol Reagent (Ambion, 15596018) according to the manufacturer's instruction. 500 ng or 1 µg of purified RNA was reverse transcribed into cDNA at 37°C for 120 min using High Capacity cDNA Reverse Transcription Kit (Applied Biosystems, 4368813) in a final volume of 20 µl. 1 µl of 4 fold-diluted cDNA was used as a template for a final volume of 20 µl. Relative expression levels were obtained by the ΔΔCt method. The expression levels of Glycine receptors, *Glra1* (Primer Bank ID (Wang et al., 2012): 31982694a1), *Glra2* (33604080a1), *Glra3* (17978252a1), *Glra4* (21040223a1), *Glrb* (31981754a1), and *Mrgprd* (15546054a1) were examined by SYBR Green-based RT-qPCR. Expression levels of *Rn18s* (Mm04277571_s1, Applied Biosystems) were used as a reference for normalization. Real-time qPCR analysis of femurs obtained from hindlimb unloaded male mice for *Rankl* (Mm00441906_m1, Applied Biosystems), *Opg* (Mm01205928_m1, Applied Biosystems) and Sost (Mm00470479_m1, Applied Biosystems) was also performed. The expression levels of mitochondrial genes, *Cat* (6753272a1), *Sod1* (12805215a1), *Sod2* (31980762a1), *Gpx1* (6680075a1), *Gpx3* (15011841a1), *Gpx5* (6754062a1), *Gpx7* (13195626a1), *Cyc* (6681095a1), *Cox4i1* (6753498a1), *Cox4i2* (16716379a1), *Atp5b* (31980648a1), *Ppargc1a* (6679433a1), *Ppargc1b* (18875426a1), *Tfam* (1575501a1), *Nfr1* (31543343a1), *Foxo1* (34328255a1), *Foxo3* (9789951a1), *Tfeb* (6755736a1), *Nfe2l1* (31982173a1) were examined by SYBR Green-based RT-qPCR. Hydrolysis probes were also used for the detection of *Gpx4* (Mm.PT.58.28460496, IDT) and *Aaprα* (Mm00440939_m1, Applied Biosystems). *Gapdh* (Mm99999915_g1) was used as a reference for normalization.

<u>*Mrgprd* siRNA transfection</u>

Cationic lipid-mediated transfections using Lipofectamine 2000 (Invitrogen) were performed according to the manufacturers' protocols. MLO-Y4 cells were plated in a 6-well tissue culture plate at a density of 2- $4x10^3$ cells/cm^2. Next day, the media were replaced with antibiotic-free growth media. A complex of *Mrgprd* DsiRNA (mm.Ri.Mrgprd.13.1, 2, 3) or universal control DsiRNA (DS NC1) in a TriFECTa RNAi Kit (IDT) and Lipofectamine 2000 was added to the cells and slightly agitated to mix. After 48-72 h at 37 °C, the cells were used for Real-time qPCR analysis to verify *Mrgprd* mRNA expression or perform cell death assay.

<u>CRISPR/Cas9 genome editing</u>

MLO-Y4 cells were seeded at the density of $1x10^4$ cells/cm^2 in 2.5%FBS/2.5%CS/α-MEM with antibiotics on a 12- or 6-well plate coated with type I collagen. Next day, change media to 2.5%FBS/2.5%CS/α-MEM without phenol red and antibiotics. The Alt-R CRISPR-Cas9 System (IDT) was used for gene editing of *Mrgprd*. Selection of two suitable target sites for Cas9 protein/gRNA ribonucleoprotein complexes (Cas9 RNPs) were chosen by using web tools, CHOPCHOP and Cas-Designer (Park et al., 2015). The target sequences are MRGPRD1:5'-GATCCAGGTCACAAGGTCCA**TGG**-3', MRGPRD2:5'-TGAGCTGCAATGGCATGCAG**AGG**-3'. *Mrgprd* specific Alt-R CRISPR crRNA and tracrRNA oligos were duplexed to form sgRNA. The sgRNA was incubated with a Cas9 nuclease (RNA Bio, CP01) to assemble the ribonucleoprotein complex, which was delivered by cationic lipid-mediated transfection (Lipofectamine CRISPRMAX Cas9 Transfection Reagent, Invitrogen, 11668-019) and incubated for 3 days. After the treatment, cells were harvested for western blot analysis or detached by trypsin-EDTA and re-seeded in a 96-well plate for cell death assay.

<u>Western-blot Analysis</u>

After 72 h transfection, the cells were washed with cold PBS twice and lysed with RIPA buffer including a protease inhibitor (Sigma-Aldrich, P8340). The cell lysate and sample buffer were mixed and boiled for 5 minutes before loading on the gel. Proteins (10 µg) were separated by SDS-PAGE at 100 V and were transferred electrophoretically to a PVDF membrane at 60 V for 3 h. The membranes were blocked in a blocking solution overnight at 4°C and incubated with the primary antibody against MRGPRD (Abcam, ab155099) at 1: 2000 dilution overnight at 4°C. The blots were incubated with a peroxidase-linked anti-rabbit secondary antibody (Thermo Fisher Scientific, 32460) at 1: 5000 for 2 h at a room temperature. Afterward, the immunoblots were visualized with an enhanced chemiluminescence (ECL) detection kit (Thermo Fisher Scientific, 32132).

The analysis of band intensity was performed using a LAS-3000 Imager (Fujifilm) and ImageJ software (NIH). β-actin (A3854, Sigma-Aldrich) at 1: 25000 dilution was used for normalization of MRGPRD.

In the case of the Western-blot analysis for catalase and GPX4, MLO-Y4 cells were incubated with 5 μM L-BAIBA or 1 mM NAC for 24 h. After treatment, the cells were processed for western blot analysis with the primary antibodies, anti-catalase (Cell Signaling Technology, D5N7V), anti-GPX4 (Abcam, ab125066) at 1:2000 dilution and anti-GAPDH (Cell Signaling Technology, 5174S) at 1:10000 dilution followed by HRP-linked anti-mouse secondary antibody (Cell Signaling Technology, 7076S). Results were visualized with the ECL reagent. Densitometry evaluation was conducted using ImageJ software.

Videos

MLO-Y4 osteocyte cells were cultured in 35mm glass bottom dishes in α-MEM with 2.5% calf serum + 2.5% FBS. The cells were stained with 500nM MitoTracker Deep Red for 20 minutes at 37°C, then washed 7X with PBS. Using a Leica SP8 confocal microscope, xyt images were taken every 30 seconds, each video consists of 20 images.

Supplemental References

Ahuja, S.S., Zhao, S., Bellido, T., Plotkin, L.I., Jimenez, F., and Bonewald, L.F. (2003). CD40 ligand blocks apoptosis induced by tumor necrosis factor alpha, glucocorticoids, and etoposide in osteoblasts and the osteocyte-like cell line murine long bone osteocyte-Y4. Endocrinology *144*, 1761-1769.

Bobba, S., Resch, G.E., and Gutheil, W.G. (2012). A liquid chromatography-tandem mass spectrometry assay for detection and quantitation of the dipeptide Gly-Gln in rat brain. Analytical biochemistry *425*, 145-150.

Bonetto, A., Andersson, D.C., and Waning, D.L. (2015). Assessment of muscle mass and strength in mice. Bonekey Rep *4*, 732.

Brotto, M.A., Nosek, T.M., and Kolbeck, R.C. (2002). Influence of ageing on the fatigability of isolated mouse skeletal muscles from mature and aged mice. Experimental physiology *87*, 77-82.

Cai, C., Masumiya, H., Weisleder, N., Matsuda, N., Nishi, M., Hwang, M., Ko, J.K., Lin, P., Thornton, A., Zhao, X., et al. (2009). MG53 nucleates assembly of cell membrane repair machinery. Nat Cell Biol *11*, 56-64.

de Paula Brotto, M., van Leyen, S.A., Brotto, L.S., Jin, J.P., Nosek, C.M., and Nosek, T.M. (2001). Hypoxia/fatigue-induced degradation of troponin I and troponin C: new insights into physiologic muscle fatigue. Pflugers Arch *442*, 738-744.

Doube, M., Klosowski, M.M., Arganda-Carreras, I., Cordelieres, F.P., Dougherty, R.P., Jackson, J.S., Schmid, B., Hutchinson, J.R., and Shefelbine, S.J. (2010). BoneJ: Free and extensible bone image analysis in ImageJ. Bone *47*, 1076-1079.

Erlebacher, A., and Derynck, R. (1996). Increased expression of TGF-beta 2 in osteoblasts results in an osteoporosis-like phenotype. J Cell Biol *132*, 195-210.

Hildebrand, T., and Ruegsegger, P. (1997). Quantification of Bone Microarchitecture with the Structure Model Index. Computer methods in biomechanics and biomedical engineering *1*, 15-23.

Jahn, K., Lara-Castillo, N., Brotto, L., Mo, C.L., Johnson, M.L., Brotto, M., and Bonewald, L.F. (2012). Skeletal muscle secreted factors prevent glucocorticoid-induced osteocyte apoptosis through activation of beta-catenin. Eur. Cell Mater *24*, 197-209.

James, R.S., Staples, J.F., Brown, J.C., Tessier, S.N., and Storey, K.B. (2013). The effects of hibernation on the contractile and biochemical properties of skeletal muscles in the thirteen-lined ground squirrel, Ictidomys tridecemlineatus. J Exp Biol *216*, 2587-2594.

Jamindar, D., and Gutheil, W.G. (2010). A liquid chromatography-tandem mass spectrometry assay for Marfey's derivatives of L-Ala, D-Ala, and D-Ala-D-Ala: application to the in vivo confirmation of alanine racemase as the target of cycloserine in Escherichia coli. Analytical biochemistry *396*, 1-7.

Kitase, Y., Barragan, L., Jiang, J.X., Johnson, M.L., and Bonewald, L.F. (2010). Mechanical induction of PGE(2) in osteocytes blocks glucocorticoid induced apoptosis through both the beta-catenin and PKA pathways. J. Bone Miner. Res *25*, 2657-2668.

Park, J., Bae, S., and Kim, J.S. (2015). Cas-Designer: a web-based tool for choice of CRISPR-Cas9 target sites. Bioinformatics *31*, 4014-4016.

Park, K.H., Brotto, L., Lehoang, O., Brotto, M., Ma, J., and Zhao, X. (2012). Ex vivo assessment of contractility, fatigability and alternans in isolated skeletal muscles. Journal of visualized experiments : JoVE, e4198.

Putty, S., Rai, A., Jamindar, D., Pagano, P., Quinn, C.L., Mima, T., Schweizer, H.P., and Gutheil, W.G. (2011). Characterization of d-boroAla as a novel broad-spectrum antibacterial agent targeting d-Ala-d-Ala ligase. Chemical biology & drug design *78*, 757-763.

Putty, S., Vemula, H., Bobba, S., and Gutheil, W.G. (2013). A liquid chromatography-tandem mass spectrometry assay for d-Ala-d-Lac: a key intermediate for vancomycin resistance in vancomycin-resistant enterococci. Analytical biochemistry *442*, 166-171.

Salmon, P.L., Ohlsson, C., Shefelbine, S.J., and Doube, M. (2015). Structure Model Index Does Not Measure Rods and Plates in Trabecular Bone. Frontiers in endocrinology *6*, 162.

Schmid, B., Schindelin, J., Cardona, A., Longair, M., and Heisenberg, M. (2010). A high-level 3D visualization API for Java and ImageJ. BMC bioinformatics *11*, 274.

Shen, J., Bronson, R.T., Chen, D.F., Xia, W., Selkoe, D.J., and Tonegawa, S. (1997). Skeletal and CNS defects in Presenilin-1-deficient mice. Cell *89*, 629-639.

Stevens, A., and Farncis, R.J. (1996). Chapter 14: Micro-organisms. In Theory and Practice of Histological Techniques, 4th ed. J.C. Bancroft, and A. Stevens, eds. (New York: Churchill Livingstone), p. 766.

Tallis, J., Higgins, M.F., Cox, V.M., Duncan, M.J., and James, R.S. (2014). Does a physiological concentration of taurine increase acute muscle power output, time to fatigue, and recovery in isolated mouse soleus (slow) muscle with or without the presence of caffeine? Can J Physiol Pharmacol *92*, 42-49.

Tallis, J., Hill, C., James, R.S., Cox, V.M., and Seebacher, F. (2017). The effect of obesity on the contractile performance of isolated mouse soleus, EDL, and diaphragm muscles. J Appl Physiol (1985) *122*, 170-181.
Thornton, A.M., Zhao, X., Weisleder, N., Brotto, L.S., Bougoin, S., Nosek, T.M., Reid, M., Hardin, B., Pan, Z., Ma, J., et al. (2011). Store-operated Ca(2+) entry (SOCE) contributes to normal skeletal muscle contractility in young but not in aged skeletal muscle. Aging (Albany NY) *3*, 621-634.
Wang, X., Spandidos, A., Wang, H., and Seed, B. (2012). PrimerBank: a PCR primer database for quantitative gene expression analysis, 2012 update. Nucleic Acids Res *40*, D1144-1149.
Wright, L.E., Harhash, A.A., Kozlow, W.M., Waning, D.L., Regan, J.N., She, Y., John, S.K., Murthy, S., Niewolna, M., Marks, A.R., et al. (2017). Aromatase inhibitor-induced bone loss increases the progression of estrogen receptor-negative breast cancer in bone and exacerbates muscle weakness in vivo. Oncotarget *8*, 8406-8419.
Zhao, X., Weisleder, N., Thornton, A., Oppong, Y., Campbell, R., Ma, J., and Brotto, M. (2008). Compromised store-operated Ca2+ entry in aged skeletal muscle. Aging Cell *7*, 561-568.

Figure S1.

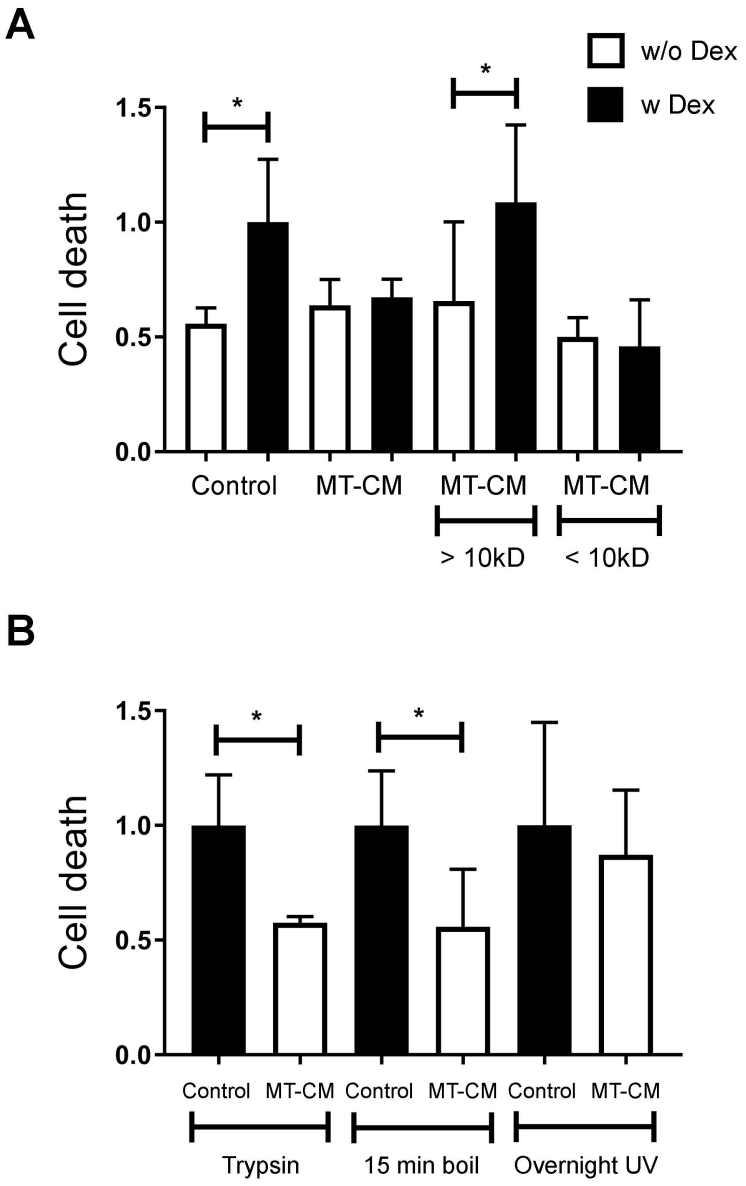

Figure S1. Low molecular weight muscle factors protect osteocytes from dexamethasone-induced cell death. Related to Figure 1.

(A) C2C12 myotube CM less than 10kD protects MLO-Y4 from cell death induced by dexamethasone. *$p<0.05$.
(B) The myotube CM retains the protective effect against cell death induced by dexamethasone after the treatment of trypsin and 15 min boiling, but not overnight UV exposure. *$p<0.05$.

Figure S2.

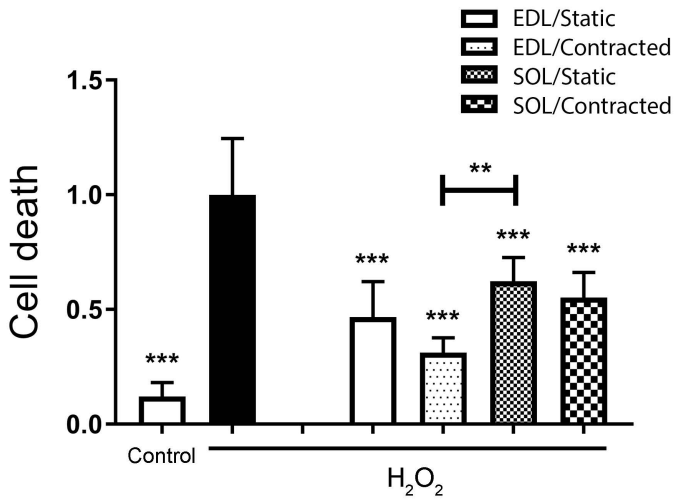

Figure S2. Both EDL and SOL secret factors that protect osteocytes from ROS-induced cell death. Related to Figure 1.

Both contracted and static EDL and SOL CMs obtained from 5-month-old male mice protect MLO-Y4 from cell death induced by H_2O_2. **p<0.01 and ***p<0.001 vs. H_2O_2.

Figure S3.

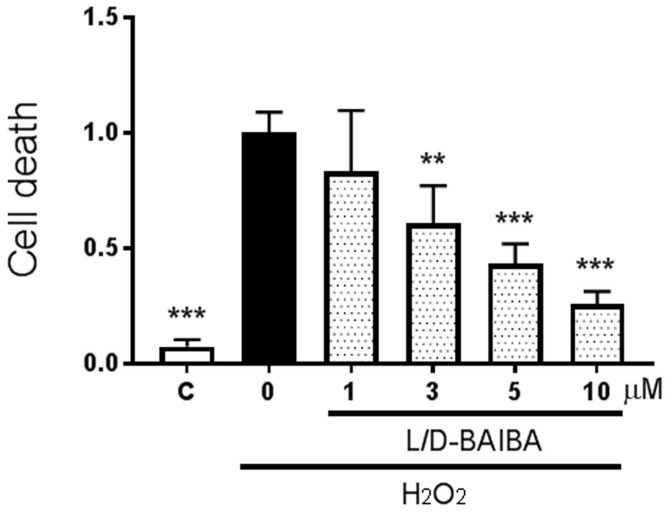

Figure S3. BAIBA protects osteoblasts from ROS-induced cell death. Related to Figure 1. BAIBA protects an osteoblast cell line, MC3T3-E1 from cell death induced by H_2O_2 in a dose-dependent manner. **p<0.01, ***p<0.001 vs. H_2O_2.

Figure S4.

A

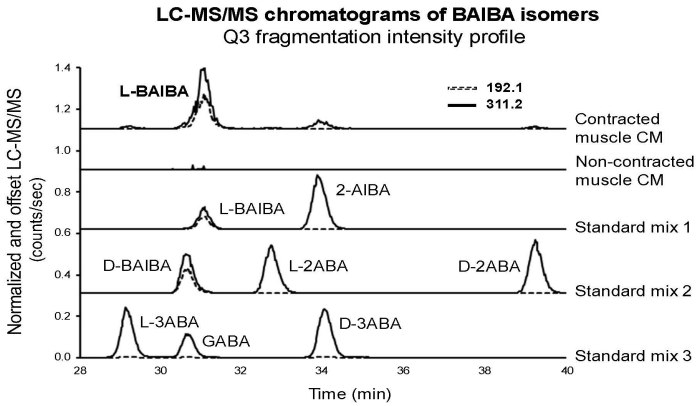

B

Amino acids in Msucle CM (μM)

Conc. (μM)	EDL 0Hz	SOL 0Hz	EDL 90Hz	SOL 90Hz
Gly	0.00	0.00	0.57	1.21
B-Ala	0.00	0.85	0.00	1.02
Ala	0.33	0.09	0.85	1.03
Arg	0.61	0.13	0.76	0.48
Asn	0.02	0.00	0.13	0.00
Asp	0.00	0.00	0.20	0.12
Gln	0.14	0.25	0.29	0.61
Glu	0.07	0.02	0.38	0.07
His	0.00	0.02	0.70	0.48
Iso	0.00	0.00	0.29	0.31
Lys	0.00	0.00	0.28	0.21
Met	0.05	0.04	0.02	0.06
Phe	0.06	0.05	0.25	0.28
Pro	0.00	0.00	0.32	0.39
Ser	0.00	0.00	0.79	0.92
Thr	0.00	0.00	0.39	0.52
Trp	0.00	0.02	0.07	0.07
Tyr	0.04	0.01	0.00	0.04
Val	0.00	0.00	0.51	0.61

** Leu was undetectable.

Figure S4. Muscle contraction increases the production of L-BAIBA, but not other isomers and amino acids. Related to Figure 5.

(A) Representative LC-MS/MS monitored chromatograms of BAIBA isomers in muscle conditioned media (top two chromatograms) and standard mixtures (bottom three chromatograms) illustrating selectivity of the Q3 = 92.1 fragment for BAIBA, and the ability to chromatographically resolve D- and L-BAIBA.

(B) Amino acids in muscle CM.

Figure S5.

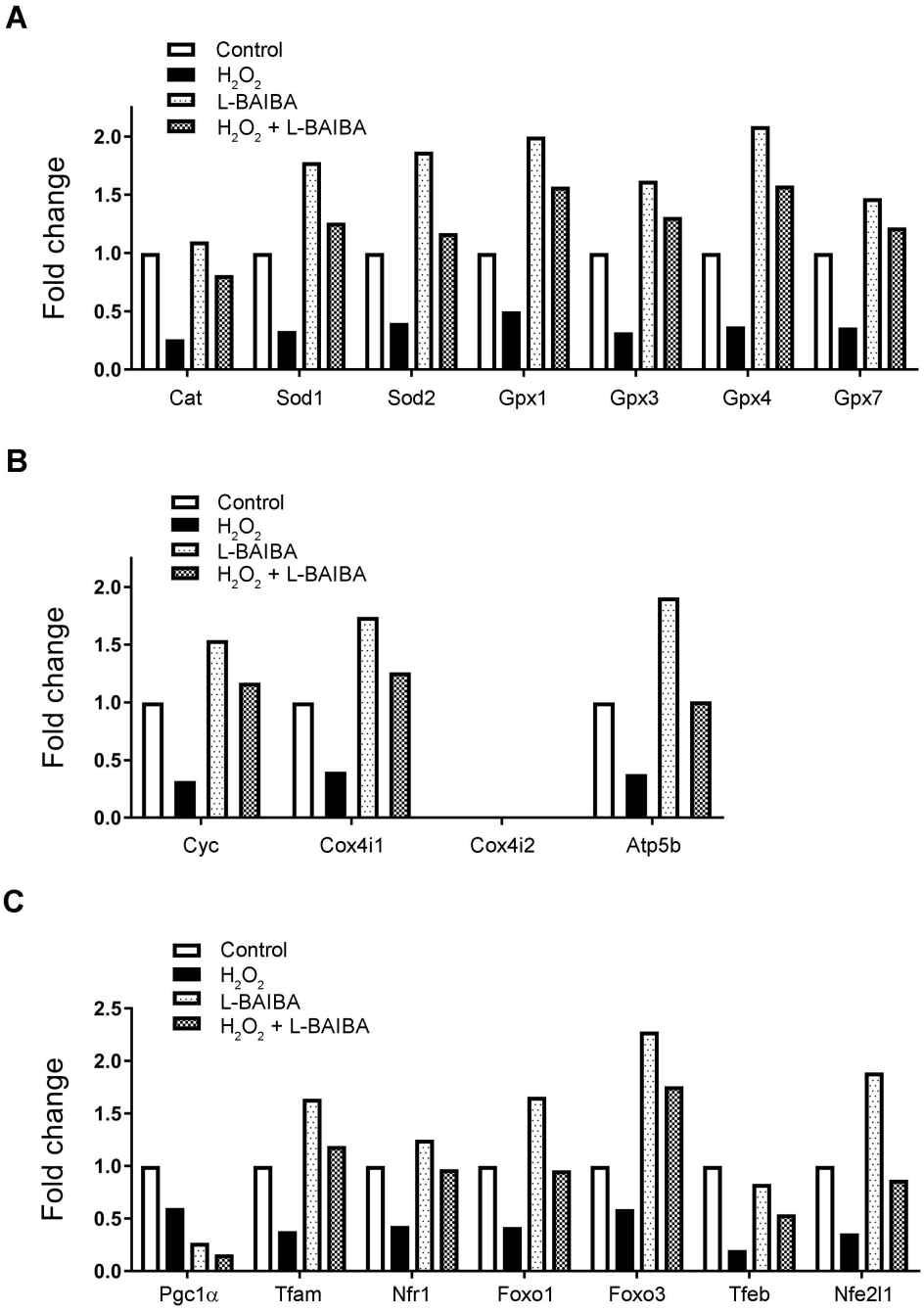

Figure S5. L-BAIBA regulates expression of mitochondrial genes. Related to Figure 7.
(A) RT-qPCR analysis of antioxidant enzyme gene expression in MLO-Y4 cells. Data are expressed as fold change over the expression level of each control. The average Ct values of the control are 27 for Cat, 23 for Sod1, 24 for Sod2, 24 for Gpx1, 27 for Gpx3, 29 for Gpx4, and 29 for Gpx7. Gpx5 is undetectable.
(B) RT-qPCR analysis of mitochondrial biogenesis-related gene expression in MLO-Y4 cells. Data are expressed as fold change over the expression level of each control. The average Ct values of the control are 21 for Cyc, 23 for Cox4i1, and 23 for Atp5b. Cox4i2 is undetectable.
(C) RT-qPCR analysis of transcriptional factor gene expression in MLO-Y4 cells. Data are expressed as fold change over the expression level of each control. The average Ct values of the control are 33 for Pgc1a, 27 for Tfam, 29 for Nfr1, 29 for Foxo1, 31 for Foxo3, 30 for Tfeb, and 26 for Nfe2l1. Pgc1b and Ppara are undetectable.